

AD-A216 527

DTIC FILE COPY

(4)

AEROSPACE REPORT NO.  
ATR-89(4752)-3

## Interfacial Chemistry of MoS<sub>2</sub> Films on Si

Prepared by

P. A. BERTRAND  
Chemistry and Physics Laboratory

10 November 1989

Laboratory Operations  
THE AEROSPACE CORPORATION  
El Segundo, CA 90245

DTIC  
ELECTE  
JAN 8 1990  
S B D

Prepared for

DEFENSE ADVANCED RESEARCH PROJECTS AGENCY  
Arlington, VA 22209



THE AEROSPACE CORPORATION

APPROVED FOR PUBLIC RELEASE;  
DISTRIBUTION UNLIMITED

90 01 08 033

## LABORATORY OPERATIONS

The Aerospace Corporation functions as an "architect-engineer" for national security projects, specializing in advanced military space systems. Providing research support, the corporation's Laboratory Operations conducts experimental and theoretical investigations that focus on the application of scientific and technical advances to such systems. Vital to the success of these investigations is the technical staff's wide-ranging expertise and its ability to stay current with new developments. This expertise is enhanced by a research program aimed at dealing with the many problems associated with rapidly evolving space systems. Contributing their capabilities to the research effort are these individual laboratories:

Aerophysics Laboratory: Launch vehicle and reentry fluid mechanics, heat transfer and flight dynamics; chemical and electric propulsion, propellant chemistry, chemical dynamics, environmental chemistry, trace detection; spacecraft structural mechanics, contamination, thermal and structural control; high temperature thermomechanics, gas kinetics and radiation; cw and pulsed chemical and excimer laser development including chemical kinetics, spectroscopy, optical resonators, beam control, atmospheric propagation, laser effects and countermeasures.

Chemistry and Physics Laboratory: Atmospheric chemical reactions, atmospheric optics, light scattering, state-specific chemical reactions and radiative signatures of missile plumes, sensor out-of-field-of-view rejection, applied laser spectroscopy, laser chemistry, laser optoelectronics, solar cell physics, battery electrochemistry, space vacuum and radiation effects on materials, lubrication and surface phenomena, thermionic emission, photo-sensitive materials and detectors, atomic frequency standards, and environmental chemistry.

Computer Science Laboratory: Program verification, program translation, performance-sensitive system design, distributed architectures for spaceborne computers, fault-tolerant computer systems, artificial intelligence, micro-electronics applications, communication protocols, and computer security.

Electronics Research Laboratory: Microelectronics, solid-state device physics, compound semiconductors, radiation hardening; electro-optics, quantum electronics, solid-state lasers, optical propagation and communications; microwave semiconductor devices, microwave/millimeter wave measurements, diagnostics and radiometry, microwave/millimeter wave thermal devices; atomic time and frequency standards; antennas, rf systems, electromagnetic propagation phenomena, space communication systems.

Materials Sciences Laboratory: Development of new materials: metals, alloys, ceramics, polymers and their composites, and new forms of carbon; non-destructive evaluation, component failure analysis and reliability; fracture mechanics and stress corrosion; analysis and evaluation of materials at cryogenic and elevated temperatures as well as in space and enemy-induced environments.

Space Sciences Laboratory: Magnetospheric, auroral and cosmic ray physics, wave-particle interactions, magnetospheric plasma waves; atmospheric and ionospheric physics, density and composition of the upper atmosphere, remote sensing using atmospheric radiation; solar physics, infrared astronomy, infrared signature analysis; effects of solar activity, magnetic storms and nuclear explosions on the earth's atmosphere, ionosphere and magnetosphere; effects of electromagnetic and particulate radiations on space systems; space instrumentation.

Aerospace Report No.  
ATR-89(4752)-3

INTERFACIAL CHEMISTRY OF  $\text{MoS}_2$  FILMS ON Si

Prepared by

P. A. Bertrand  
Chemistry and Physics Laboratory

10 November 1989

Laboratory Operations  
THE AEROSPACE CORPORATION  
El Segundo, CA 90245

Prepared for

DEFENSE ADVANCED RESEARCH PROJECTS AGENCY  
Arlington, VA 22209

APPROVED FOR PUBLIC RELEASE;  
DISTRIBUTION UNLIMITED


Report No.  
ATR-89(4752)-3

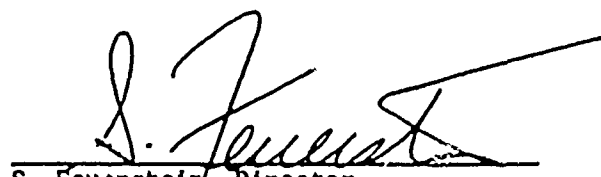
INTERFACIAL CHEMISTRY OF  $\text{MoS}_2$  FILMS ON Si

Prepared

  
P. A. Bertrand

Approved

  
H. K. A. Kan, Head  
Surface Science Department

  
S. Feuerstein, Director  
Chemistry and Physics Laboratory

# ABSTRACT

The interface between rf-sputter-deposited  $\text{MoS}_2$  films and single-crystal Si was studied by observing thin ( $<100 \text{ \AA}$ ) films with electron energy loss spectroscopy, Auger electron spectroscopy, and x-ray photoelectron spectroscopy. The interface is not atomically smooth; it is a broad and chemically complex region. The surface of the native oxide ( $\text{SiO}_2$ ) is sulfated by the plasma. The initial  $\text{MoS}_2$  in films deposited at  $220^\circ\text{C}$  is chemically the same as crystalline  $\text{MoS}_2$ ; that is, there is no chemical bonding between the film and the substrate. There is evidence that the initial  $\text{MoS}_2$  in films deposited at  $70^\circ\text{C}$  is chemically bonded to the crystal, perhaps through Mo-S-O or Mo-O linkages. (A11)



Accession For	
NTIS GRA&I	<input checked="" type="checkbox"/>
DTIC TAB	<input type="checkbox"/>
Unannounced	<input type="checkbox"/>
Justification	
By _____	
Distribution/	
Availability Codes	
Dist	Avail and/or Special
A-1	

## ACKNOWLEDGMENTS

The author thanks R. Bauer for preparing the samples, S. A. Jackson for performing the AES and EELS measurements, and J. L. Childs for performing the XPS measurements.

Funding for this effort was processed through Space Systems Division Contract No. FO4701-88-C-0089 under an Interagency Agreement from the Defense Advanced Research Projects Agency.

## CONTENTS

ABSTRACT .....	v
ACKNOWLEDGMENTS.....	vii
I. INTRODUCTION.....	1
II. EXPERIMENTAL.....	5
III. RESULTS AND DISCUSSION.....	7
A. Reference Materials.....	7
B. Thick MoS <sub>2</sub> Films.....	7
C. Thin HT Films.....	13
D. Thin AT Films.....	18
IV. CONCLUSIONS.....	21
REFERENCES.....	23

## FIGURES

1.	Molybdenum Disulfide Crystal Structure.....	2
2.	FEL Spectra of Reference Materials.....	8
3.	Schematic Energy-Level Diagram for MoS <sub>2</sub> .....	9
4.	EEL Spectra of Thick HT MoS <sub>2</sub> Films.....	12
5.	EEL Spectra of Thick PT MoS <sub>2</sub> Films.....	14
6.	EEL Spectra of Thick AT MoS <sub>2</sub> Films.....	15
7.	EEL Spectra of Thin HT MoS <sub>2</sub> Films.....	17
8.	EEL Spectra of Thin AT MoS <sub>2</sub> Films.....	19

## TABLE

1.	S/Mo Ratios for MoS <sub>2</sub> .....	10
----	--	----



## I. INTRODUCTION

The adhesion of thin films to their substrates is an important factor in their use in electronics, corrosion prevention, and lubrication. In particular, adhesion may be the critical parameter that determines the wear life of solid lubricant films; it has been suggested that films fail when they are pushed out of the wear track. Systems with chemical bonds across the interface will have enhanced adhesion over systems in which only van der Waals interactions are operative. Covalent materials, such as the important engineering ceramics SiC and  $\text{Si}_3\text{N}_4$  and the solid lubricant  $\text{MoS}_2$ , have strong directional bonds. If the same kind of bonds could be formed between such materials, a strongly adhesive lubricant-substrate system should result,

SiC has a structure in which each Si atom is tetrahedrally coordinated to four C atoms, and each C atom is tetrahedrally coordinated to four Si atoms. In  $\text{Si}_3\text{N}_4$ , the Si coordination is tetrahedral, but each N atom is trigonally coordinated to three Si atoms. At the clean surface of each of these materials there are unsatisfied, dangling bonds. Under normal atmospheric conditions, these bonds are satisfied by oxygen to form the native oxide:  $\text{SiO}_2$  in the case of SiC, and an oxynitride enriched in  $\text{SiO}_2$  at the surface in the case of  $\text{Si}_3\text{N}_4$ . In this study, single-crystal Si was used as a substrate, because it also has  $\text{SiO}_2$  native oxide and does not have the complex microstructure and reactive grain boundaries of true engineering ceramics.

In the crystal structure of  $\text{MoS}_2$ , illustrated in Figure 1, each S-Mo-S sandwich is tightly bound internally and interacts with neighboring sandwiches only through van der Waals forces. The plane between sandwiches, then, is a plane of easy shear. However, since there are no vacant orbitals or dangling bonds on the basal plane, there is no possibility of strong chemical bonding between the basal plane of a crystallite and another surface. Thus a crystallite with parallel orientation (as it will be called in this report) will not adhere well to a substrate. At the edges of a crystallite perpendicular to the basal plane there will be unsatisfied bonds: S atoms,

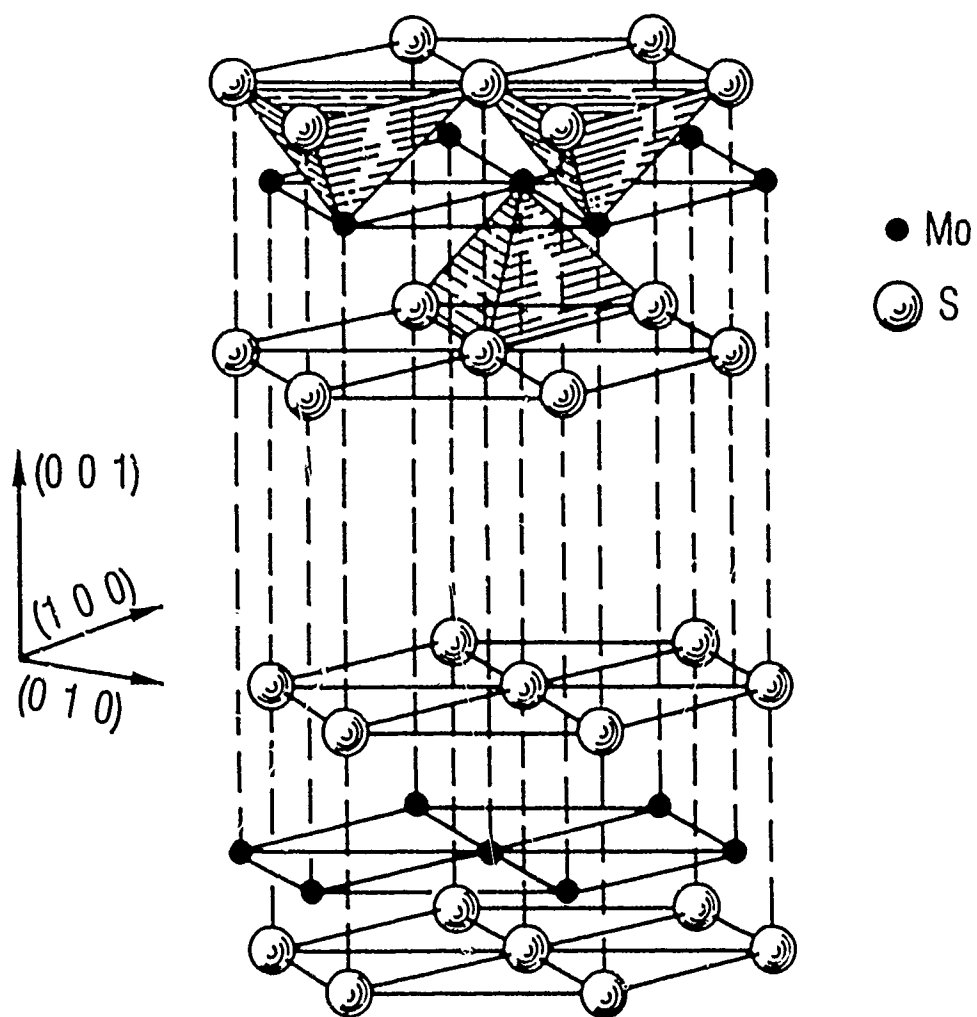
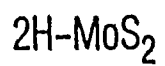


Fig. 1. Molybdenum Disulfide (MoS<sub>2</sub>) Crystal Structure

for instance, that are missing their neighboring Mo atom. Such bonds may be satisfied by oxygen or other impurities, or by the substrate. If they are satisfied by the substrate, the crystallite will be forced to align with its basal plane perpendicular to the substrate because of the directionality of the S dangling bonds: They point to where the missing Mo ought to be.

In the experiments reported here, very thin ( $<100 \text{ \AA}$ ) films of  $\text{MoS}_2$  were rf-sputter-deposited onto Si and observed by electron energy loss spectroscopy (EELS) to determine the presence and identity of interfacial bonds. Thick films (2000 and 10,000  $\text{\AA}$ ) were also studied to characterize the surfaces of the films and compare them to molybdenite crystal, molybdenum trioxide, and the thin films. The spectra of the thin films are not mere superpositions of substrate and molybdenite spectra; there is much interesting chemistry occurring at the interface.

Electron energy loss spectroscopy is a powerful method for observing chemical bonds. A low-energy electron beam (200 eV in these experiments) is reflected from a surface. Most of the electrons are reflected elastically; a certain number undergo inelastic collisions with the surface during reflection. The important inelastic process for this study is the transfer of energy from a beam electron to a valence-band electron in the solid surface, resulting in the latter's promotion to an unoccupied orbital in the conduction band. The amount of energy lost by the beam electron is then just the energy difference between the conduction-band and valence-band states involved in the transition. EELS is thus a direct probe of the bonding electrons, as is ultraviolet photoelectron spectroscopy, not an indirect one, as is x-ray photoelectron spectroscopy (XPS).

## 17. EXPERIMENTAL

Single-crystal silicon, (100) or (111) orientation, was selected as a model substrate for the important engineering ceramics SiC and Si<sub>3</sub>N<sub>4</sub>. The specimens were ultrasonically cleaned in methanol before deposition. Films of MoS<sub>2</sub> were prepared with an rf diode-sputtering apparatus operating at 2 kW with a frequency of 13.56 MHz and an argon pressure of  $2 \times 10^{-2}$  torr. The 152.4-mm-diam MoS<sub>2</sub> target was hot-pressed from powder (99% pure) and was bonded to a copper plate. The specimens to be coated were located 36 mm below the target on a ground block that could be heated. The chamber was evacuated to a pressure of  $1-2 \times 10^{-6}$  torr before sputtering, then filled to  $2 \times 10^{-2}$  torr with argon. The target was conditioned by presputtering onto a shutter over the samples for 2 hr. The shutter was opened briefly (several seconds or less) for deposition of the very thin films. The sputtering rate was  $\sim 200$  Å/min for an rf power density of 2 W/cm<sup>2</sup>. The films discussed here are <100 Å thick, 2000 Å thick, and 10,000 Å thick. Two temperature regimes were used for thin-film deposition: With no temperature control, at the ambient temperature in the chamber (60-70°C); the films are designated AT films. The second regime was at high temperature, 220°C; the films are designated HT films. Thick films were also produced at ambient temperature after the substrate was pretreated at 220°C in situ; these are called PT films. SEM micrographs have been taken of these films and other films prepared by the same methods in our laboratory. The results were published previously.<sup>1</sup> All the films have a "wormlike" microstructure. AT and PT films are more densely packed than HT films. The thin films are too thin to observe by SEM. TEM studies have been made, and the results have been published elsewhere.<sup>2</sup>

Coated specimens were transferred immediately to a vacuum desiccator and ultimately to a scanning Auger microprobe within a few days. Thin AT films (which were expected to be more sensitive to oxidation) were always loaded directly into the microprobe with no storage time. Some thick films were observed after several months' storage to determine the effect of oxidation on the EEL spectra. Two reference samples were also examined. Molybdenite

crystal (from Ward's Scientific Establishment) was cleaved in air immediately before loading. No C and very little O were observed on this surface by AES or XPS. Mo foil was used as a reference for oxidized Mo: Our sample was determined to be entirely  $\text{MoO}_3$  in the surface layers sampled by XPS. EELS and Auger electron spectroscopy (AES) were performed in the microprobe; XPS also was carried out on most samples in a McPherson ESCA-36 spectrometer.

A low-energy electron gun was added to the scanning Auger microprobe for the EELS experiments. The sample was placed at the focal point of the cylindrical mirror analyzer by the usual procedures, and the low-energy electron beam was directed onto the analysis area by a mechanical system with a bellows. The EEL spectra were detected as the second derivative of the electron current with respect to voltage. This is the standard method and sharpens the peaks at the expense of quantitative intensity analysis. The full width at half-maximum of the elastic peak is 1.1 eV for a peak energy of 200 eV and is limited by the spread in energy of the electrons produced by the gun.

### III. RESULTS AND DISCUSSION

#### A. REFERENCE MATERIALS

The EEL spectra of two reference samples are shown in Figure 2. Our results for molybdenite crystal (Fig. 2a) agree well with previous literature results: loss peaks at 3.5, 5.3, and 8.5 eV corresponding to valence band-conduction band transitions; a peak at 13 eV due to promotion of an S(3s) core electron to the conduction band, and peaks at higher loss energy due to plasmon excitations.<sup>3-5</sup> A schematic energy-level diagram for MoS<sub>2</sub> (Fig. 3) shows the transitions that are responsible for specific losses; not all the transitions are fully resolved.<sup>3</sup> The peak at 3.5 eV is due to promotion of a Mo d<sub>z2</sub> electron (a<sub>1</sub>' molecular orbital) to the lowest level of the conduction band. The peak at 5.3 eV could then be due to the promotion of an e'' electron to the lowest conduction level or an a<sub>1</sub>' electron to the upper conduction level. The peak at 8.5 eV is due to the promotion of an a<sub>2</sub>'' electron to the upper conduction level or an a<sub>1</sub>' (Mo 5s) electron to the lower conduction level.

The native oxide on our sample of Mo foil is MoO<sub>3</sub>, which is also the final product of oxidation of MoS<sub>2</sub> films. The coordination of the Mo is octahedral but distorted. The EEL spectrum of oxidized Mo (Fig. 2b) exhibits a major peak at 4.6 eV, probably due to promotion of nonbonding O(2p) electrons to the conduction band. The peaks at 10.6 and 13.5 eV are assigned to promotion of bonding electrons from the E<sub>g</sub> and T<sub>1u</sub> levels [Mo(p, d<sub>z2</sub>, d<sub>x2-y2</sub>) levels combined with bonding O(2p) levels] to the conduction band.

#### B. THICK MoS<sub>2</sub> FILMS

The compositions of the MoS<sub>2</sub> films were measured by AES and XPS. In the Auger spectra, there are two sets of S and Mo peaks: S(LMM) at 151 eV and Mo(MNN) at 186 eV, and S(KLL) at 2117 eV and Mo(LMM) at 2044 eV. The large energy difference between these two sets results in a large difference in the inelastic mean free path of the electrons produced by the transitions. It permits different depths into the specimen to be sampled by the two sets,

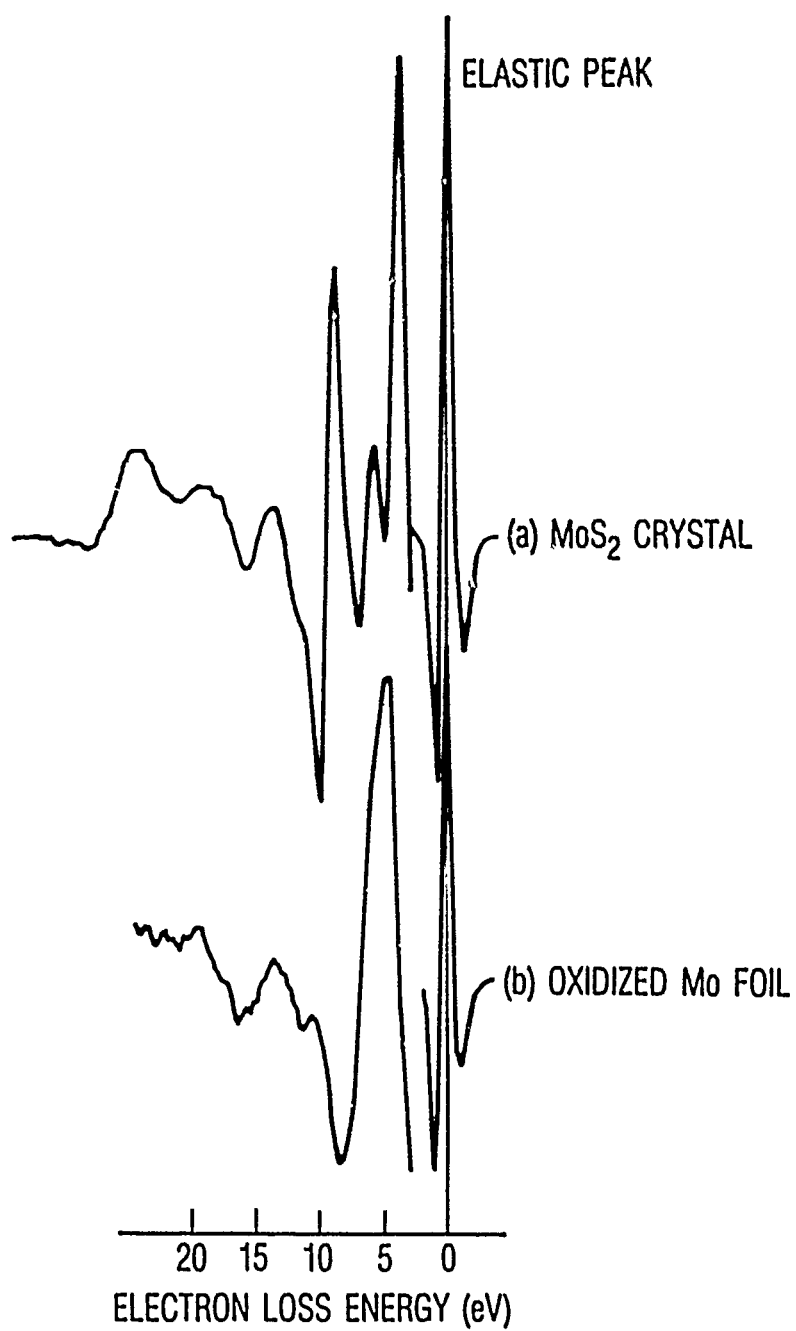


Fig. 2. EEL Spectra of Reference Materials

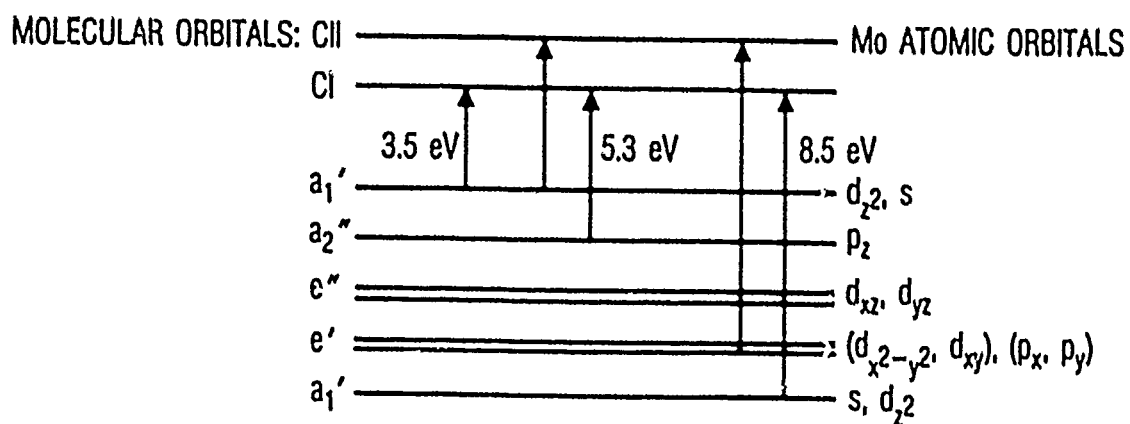


Fig. 3. Schematic Energy-Level Diagram for MoS<sub>2</sub>



-43 Å for the high-energy set and -12 Å for the low-energy set.<sup>6</sup> The XPS peaks for S(1s) at 164-eV binding energy (1090-eV kinetic energy) and Mo(3d) at 234-eV binding energy (1020-eV kinetic energy) sample about 32 Å into the surface.<sup>6</sup> XPS can also detect oxidation of the surface by the chemical shift of the Mo peak from Mo IV to Mo VI as MoS<sub>2</sub> oxidizes to MoO<sub>3</sub>. This process has been observed before,<sup>1,7</sup> but, within the detection limits of the XPS, no oxidation was present on the samples discussed here. A small amount of oxygen was detected on all the samples by both XPS and AES.

The S/Mo ratios measured for thick rf-sputtered films on Si are given in Table 1. The values for crystalline molybdenite (the average for 13 samples) are included for comparison. No corrections have been made for cross-section or spectrometer sensitivity. The AES ratios were calculated from peak-to-peak heights in the first-derivative spectra; the XPS ratios were calculated from peak areas as determined by cutting the peaks out of paper and weighing them. The thick-film measurements are averages for 11 samples each for HT and AT films and for 8 samples for PT films. The error figures are the standard deviations from the averages. The XPS results imply that the films are

Table 1. S/Mo Ratios for MoS<sub>2</sub>

	S/Mo (Low-Energy AES)	S/Mo (High-Energy AES)	S/Mo (XPS)
Crystal	8.6 ± 0.4	1.7 ± 0.1	0.52
Thick AT films	9.3 ± 0.8	1.4 ± 0.2	0.51 ± 0.04
Thick HT films	8.6 ± 0.4	1.3 ± 0.1	
Thick PT films	8.9 ± 0.8	1.4 ± 0.2	

stoichiometric in S and Mo; the AES results suggest that the surfaces are S-rich while the bulk is S-poor. There are two possible explanations for this discrepancy. One is that electron-beam damage is occurring in the Auger spectrometer, resulting in a sulfur gradient in the surface layers for these measurements, although the films are originally stoichiometric as observed in XPS. Additional experiments using varying beam currents and long exposure times show no such changes. Another possibility is that the films are indeed S-rich at the surface ( $\sim 12 \text{ \AA}$ ), stoichiometric when deeper layers are averaged in ( $\sim 32 \text{ \AA}$ ), and S-poor in the bulk ( $\sim 43 \text{ \AA}$  and presumably deeper).

EEL spectra for thick  $\text{MoS}_2$  films produced at  $220^\circ\text{C}$  (HT) on Si are depicted in Figure 4. The EEL spectrum for a  $2000\text{-\AA}$ -thick, fresh film (Fig. 4a) is almost exactly like that of  $\text{MoS}_2$  crystal: three major peaks at 3.5, 5.3, and 8.5 eV. In addition, there are minor peaks at 4.5, 6.8, and 9.8 eV due to elemental sulfur,<sup>8</sup> as predicted above. (The 9.8-eV peak is not visible in Fig. 4a, perhaps because of the steep falloff of the 8.5-eV  $\text{MoS}_2$  peak.) After several months of storage in a vacuum desiccator, the film has changed (Fig. 4b). The  $\text{MoS}_2$  and S peaks are still visible in the EEL spectrum, but a new peak at 10.6 eV has appeared, and the valley at  $\sim 4.5 \text{ eV}$  has completely filled in. Both locations are where losses due to  $\text{MoO}_3$  appear. There are also changes in the spectrum at  $\sim 6 \text{ eV}$ , where one expects losses due to sulfate species. It is reasonable to conclude that oxidation has begun at the topmost surface of the sample. EELS will be much more sensitive to detecting such oxidation than XPS because its analysis depth is shallower ( $14 \text{ \AA}$  vs.  $32 \text{ \AA}$  mean free path), and the bonding electrons are observed directly and not by their effect on lower core levels.

According to this explanation of the stored  $2000\text{-\AA}$ -thick film spectrum, the fresh  $10,000\text{-\AA}$ -thick film is already oxidized (Fig. 4c). Its spectrum is essentially equivalent to that of the stored, oxidized film. (One must bear in mind that the relative intensities of second-derivative peaks are heavily influenced by the shape of the original peak and are thus not good indicators of the number of absorbers.) The fresh  $10,000\text{-\AA}$  film was made in the same deposition run as the fresh  $2000\text{-\AA}$  film, so the amount of oxygen in the films is the same. The reason for this apparent quick oxidation is the different

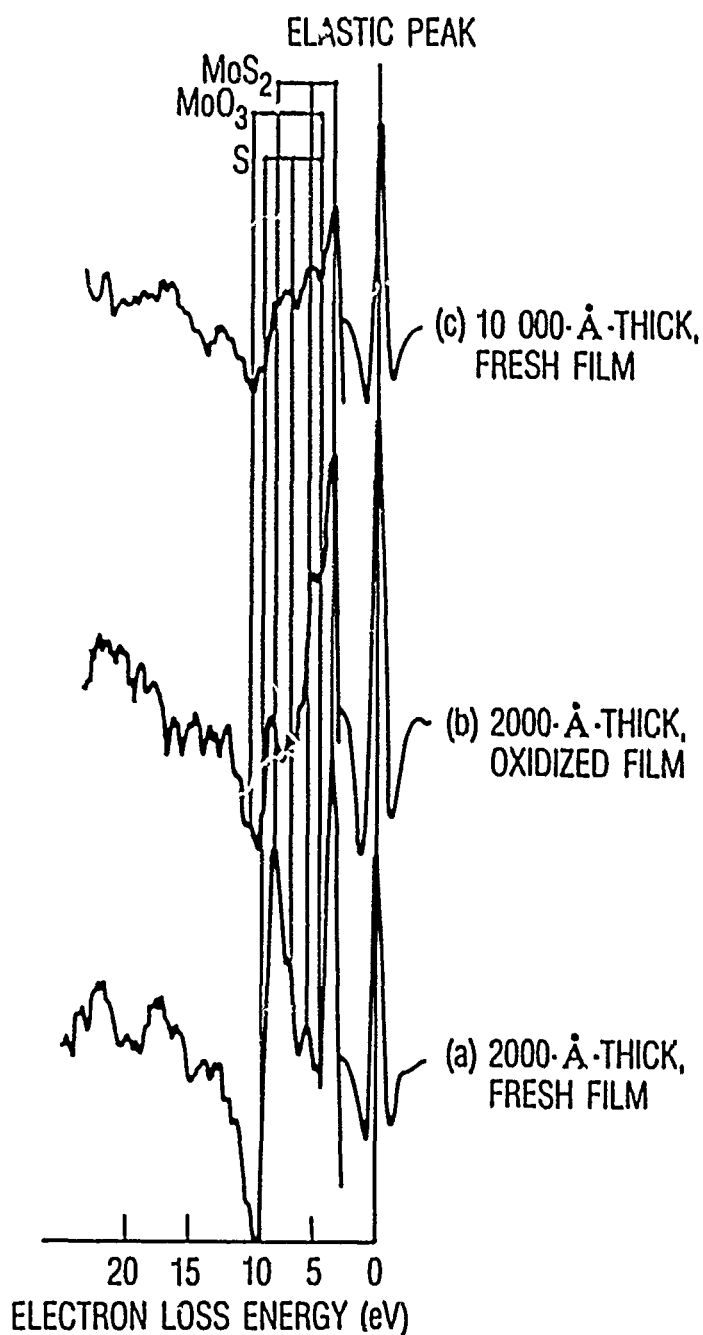


Fig. 4. EEL Spectra of Thick HT  $\text{MoS}_2$  Films.  $\text{MoS}_2$  peaks occur at 3.5, 5.3, and 8.5 eV; S peaks occur at 4.5, 6.8, and 9.8 eV;  $\text{MoO}_3$  peaks occur at 4.5 and 10.6 eV; and sulfate peaks occur at -6 eV.

crystallite orientation at the surface of the 2000- and 10,000-Å-thick HT films.<sup>9</sup> In 10,000-Å-thick HT films, the upper ~8000 Å of crystallites are perpendicular to the substrate, and the more reactive edge surface is exposed. This surface reacts with oxygen immediately either in the deposition chamber or during transfer of the sample from the deposition chamber to the analysis chamber; therefore, the surface observed by EELS is essentially oxidized. On the other hand, in 2000-Å-thick HT films, the crystallites are parallel to the substrate, and the less reactive basal surface is exposed. The edge surfaces will adsorb and react with oxygen, but only a small fraction of the surface consists of such edges. Only after several months has enough oxidation taken place to disrupt the surface crystallites and be visible in EELS.

The EEL spectra for thick PT films (Fig. 5) are the same as for the HT films. The spectra for the 2000-Å-thick films are MoS<sub>2</sub>-like, with some S at the surface (almost none is visible for the sample spectrum shown in Fig. 5a), and the 10,000-Å-thick films are oxidized at the surface due to the exposure of edge planes. Because both PT and HT films are oriented parallel to the substrate in the first 2000 Å, and perpendicular above that, these results are not surprising.

Ambient-temperature (AT) films have crystallites that are oriented perpendicular to the substrate even when 2000 Å thick. Thus the EEL spectra from the 2000- and 10,000-Å-thick AT films (Fig. 6) have all the same peaks: those due to MoS<sub>2</sub>, MoO<sub>3</sub>, and S, although the intensities are different. All peaks are characteristic of the oxidized edge plane surface.

### C. THIN HT FILMS

Thin HT films on Si were made by exposing the substrates to the deposition plasma for several seconds or less using a mechanical shutter. Several samples had no observable S or Mo signals in either XPS or AES. Those exposed slightly longer had S but no Mo. Increasing exposure left Mo on the surface, and the S/Mo ratio tends toward that of the thick films as exposure increases. The S XPS spectra show a broad Gaussian peak, which indicates the unresolved

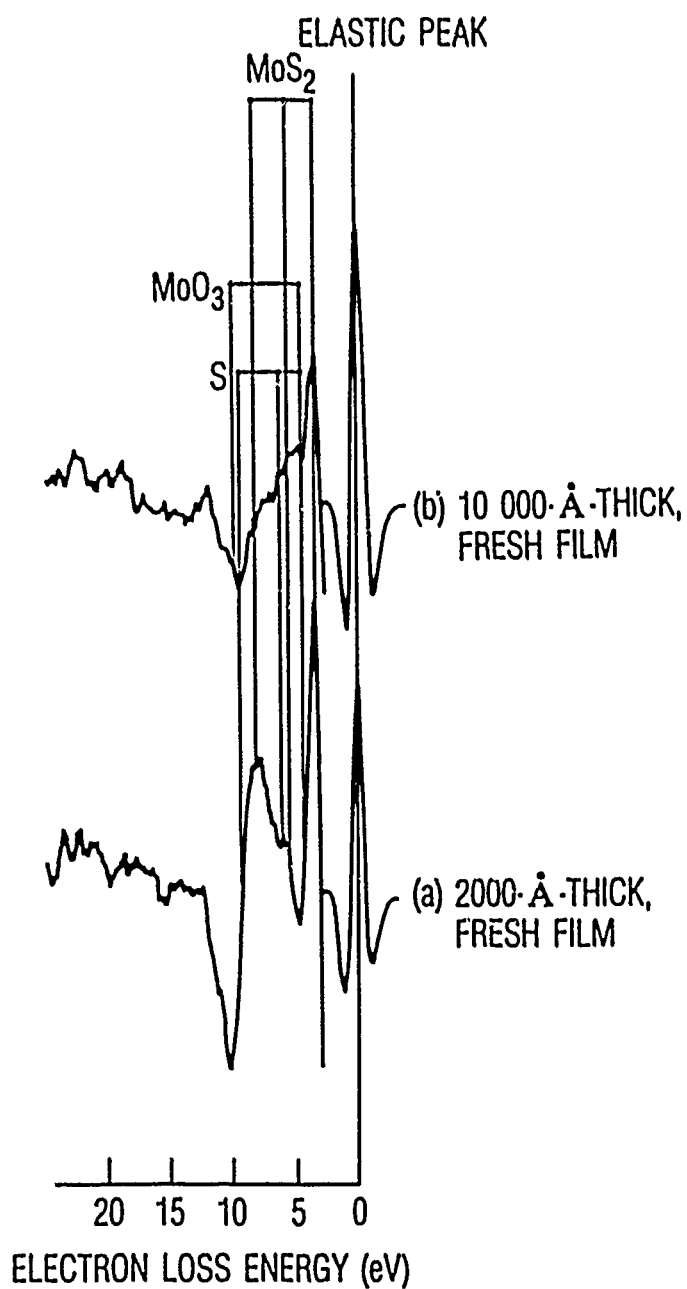


Fig. 1

EEL Spectra of Thick PT MoS<sub>2</sub> Films. MoS<sub>2</sub> peaks occur at 3.5, 5.3, and 8.5 eV; S peaks occur at 4.5, 6.8, and 9.8 eV; MoO<sub>3</sub> peaks occur at 4.5 and 10.6 eV; and sulfate peaks occur at -6 eV.

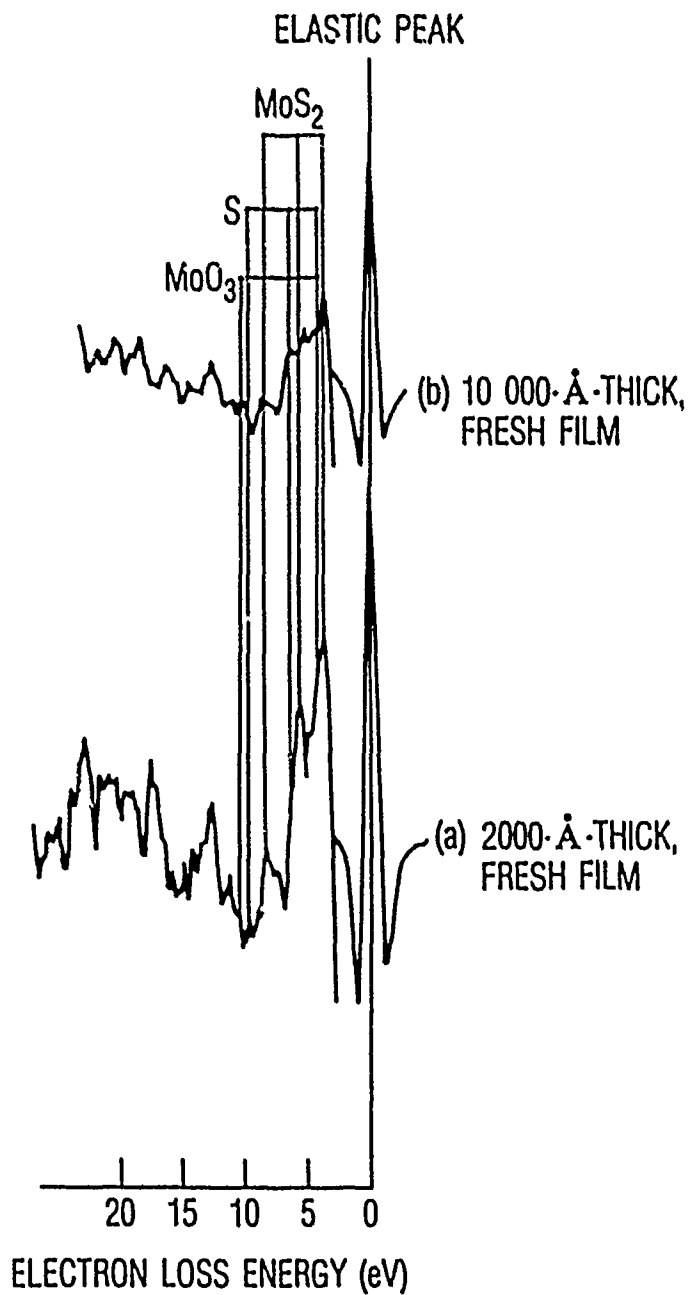


Fig. 6. EEL Spectra of Thick AT MoS<sub>2</sub> Films. MoS<sub>2</sub> peaks occur at 3.5, 5.3, and 8.5 eV; S peaks occur at 4.5, 6.8, and 9.8 eV; MoO<sub>3</sub> peaks occur at 4.5 and 10.6 eV; and sulfate peaks occur at -6 eV.

presence of both elemental and sulfide sulfur. The thickness for these very thin films cannot be estimated because the films are not chemically homogeneous and are probably patchy; even exposure time is only a rough estimate because of the experimental technique. The films can be ordered on the basis of their S/Si ratios in either XPS or AES, and also by the changes in EELS discussed below. All three of these methods independently give generally the same ordering of the 26 samples. Films with higher S/Si ratios will be called "thicker" for convenience, since a smooth, continuous film that was actually thicker would have a higher ratio.

The EEL spectra of the thin HT films can be grouped into eight categories that are dependent on thickness (Fig. 7). The category 1 films (Fig. 7a) have no S or Mo present in their XPS or AES spectra, although they were exposed to the plasma for a fraction of a second. The EEL spectra are characteristic of  $\text{SiO}_2$ :<sup>10</sup> a peak at 10.3 eV due to nonbonding O(2p) excitations, and a peak at 13.0 eV due to Si-O  $\sigma$ -bond excitations. Peaks at higher loss are well described by the  $\text{SiO}_2$  dielectric function, and the three peaks at 3.3, 5.0, and 6.7 eV are due to surface states of amorphous  $\text{SiO}_2$ . The Si substrates were covered with native oxide and were not etched before  $\text{MoS}_2$  deposition.

The second category of EEL spectra (Fig. 7b) shows a loss appearing at ~6 eV in addition to the  $\text{SiO}_2$  losses that can still be observed. It is probably due to S-O bonding, and S is the only other element present in XPS and AES. In several XPS spectra a sulfate peak is visible, but with very low signal-to-noise ratio. The S/Si AES ratios (calculated from peak-to-peak heights with no corrections for sensitivity) are <1. The third category (Fig. 7c) is quite similar, although traces of Mo are present in XPS and AES and the S/Si AES ratios are between 3 and 5. There is no evidence of Mo-O bonding, which would cause losses at 4.6 and 10.6 eV. The fourth category (Fig. 7d) again is essentially  $\text{SiO}_2$  with sulfates. The S/Si AES ratios are between 5 and 10.

With the fifth category (Fig. 7e),  $\text{MoS}_2$  losses begin to appear and those of  $\text{SiO}_2$  disappear. The S/Si AES ratios are between 7 and 20 for category 5, 7 and 50 for category 6, 20 and 50 for category 7, and are greater than 60 for

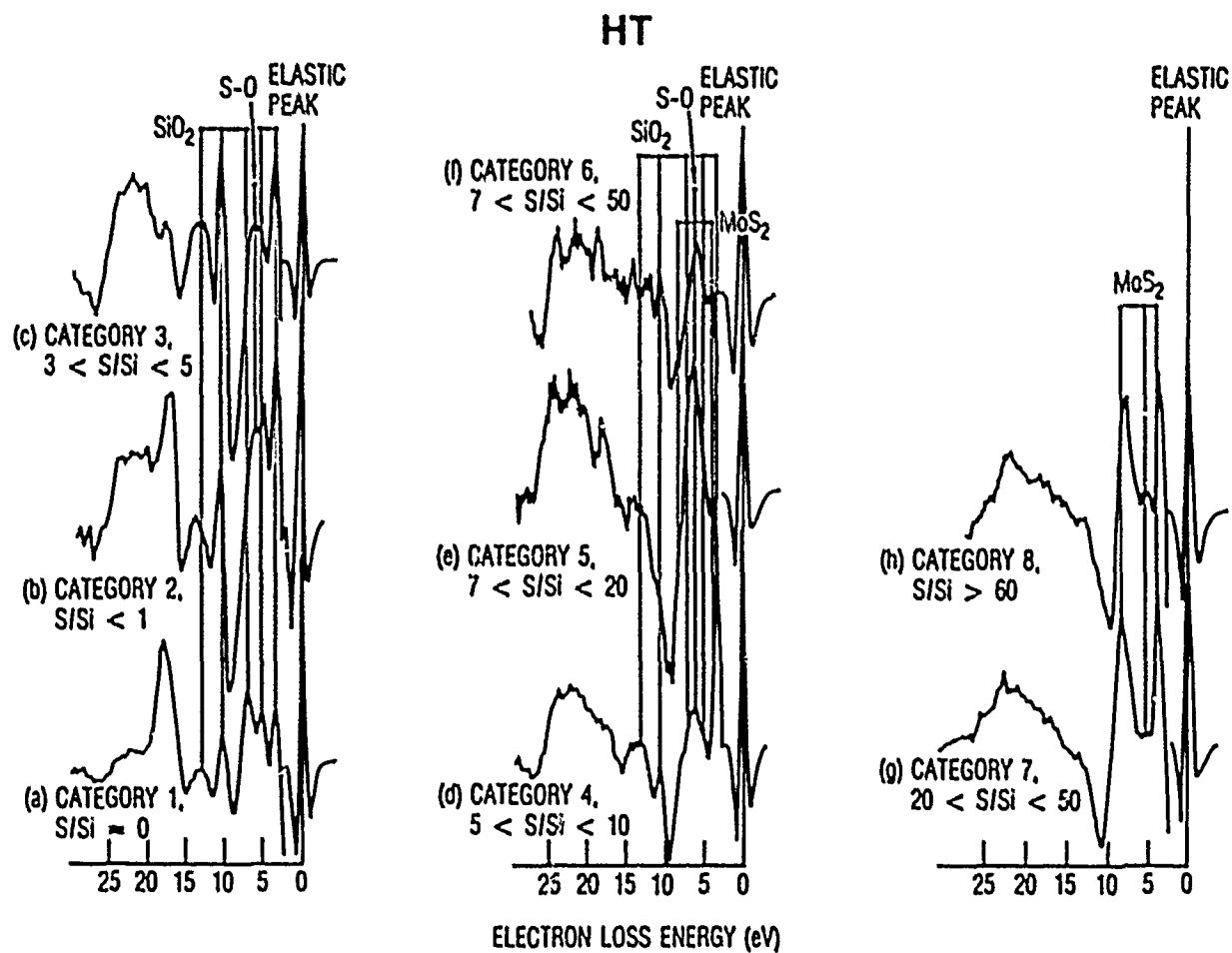


Fig. 7. EEL Spectra of Thin HT  $\text{MoS}_2$  Films.  $\text{MoS}_2$  peaks occur at 3.5, 5.3, and 8.5 eV;  $\text{SiO}_2$  peaks occur at 3.3, 5.0, 6.7, 10.3, and 13.0 eV; and sulfate peaks occur at -6 eV.



category 8. The sulfate loss at 6 eV remains prominent until category 7 (Fig. 7g). In categories 5 through 8, the losses due to  $\text{MoS}_2$  transitions occur at the same energies as those of the crystal, indicating that the initial  $\text{MoS}_2$  formed is unaffected energetically by the substrate; that is, there are no strong chemical bonds between the  $\text{MoS}_2$  and the substrate. This lack is corroborated by previous x-ray diffraction results,<sup>9</sup> which show that thin HT films are oriented parallel to the substrate. Thus the unreactive basal plane is next to the substrate, which precludes formation of strong chemical bonds between the Si and  $\text{MoS}_2$ .

#### D. THIN AT FILMS

The EEL spectra of the 13 thin AT films can be separated into seven categories (Fig. 8). These categories do not necessarily correspond in thickness (or S/Si ratios) to those of the HT films. The films of the first category have no S or Mo in their XPS or AES spectra. Their EEL spectra (Fig. 8a) are characteristic of  $\text{SiO}_2$ , just as in the category 1 thin HT films. The surface states are different on these AT substrates. The two surface states at highest loss energy are at the same energies as those of the HT substrate (5.0 and 6.7 eV), but the lowest loss peak on the AT substrates is at 4.5 eV instead of 3.3 eV. The shape of the spectra in this region is not as well defined for the AT substrate as for the HT substrate, probably because the surface is covered with more -OH groups with their interactions broadening the energy levels.

The spectra of the second category of AT films, which have S/Si AES ratios less than 1 (Fig. 8b), indicate the presence of some sulfates at ~6 eV. In addition, a 3.3-eV loss, which can be associated with electrons in a surface state of  $\text{SiO}_2$  as in the HT films, has appeared. Adding a little S to the surface has changed the surface states by reaction, but unfortunately the resolution of the present EEL spectrometer is not sufficient to examine the reaction products in detail. Of course, the states may be so broad that increased resolution may not help.

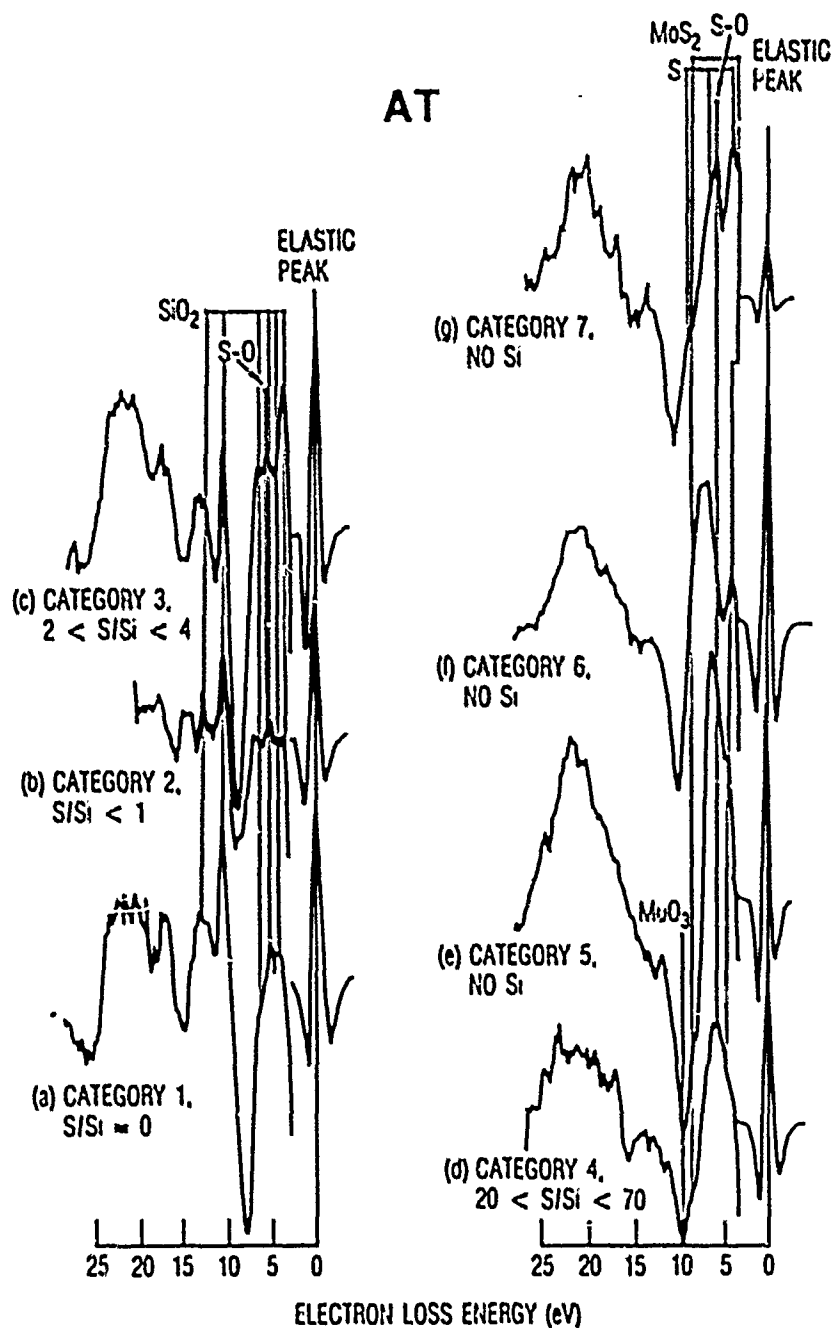


Fig. 8. EEL Spectra of Thin AT MoS<sub>2</sub> Films. MoS<sub>2</sub> peaks occur at 3.5, 5.3, and 8.5 eV; SiO<sub>2</sub> peaks occur at 3.3, 4.5, 5.0, 6.7, 10.3, and 13.0 eV; sulfate peaks occur at -6 eV; S peaks occur at 4.5, 6.8, and 9.8 eV; and MoO<sub>3</sub> peaks occur at 4.5 and 10.6 eV.

The third category of AT films (Fig. 8c) looks very much like the third category of HT films (Fig. 7c):  $\text{SiO}_2$  with sulfates. The S/Si AES ratios are between 2 and 4. In the EEL spectra of the category 4 AT films (Fig. 8d), the  $\text{SiO}_2$  substrate is not visible. Sulfates appear to be the major components of the surface, although elemental S (4.5, 6.8, and 9.8 eV) could be present, as could  $\text{MoO}_3$  (4.6 and 10.6 eV). Again, the resolution of these spectra is not sufficient to be more conclusive. The S/Si AES ratios are between 20 and 70.

$\text{MoS}_2$  loss peaks begin to appear in the spectra of category 4 films (Fig. 8d), and progressively grow in (Figs. 8e, f, and g). No Si is visible in the AES spectra of films in these categories. The sulfate loss peak remains strong, however, unlike that of the HT films. Elemental S can be present in large amounts, as in the spectrum shown for category 7 (Fig. 8g). An interesting observation can be made about the 3.5-eV  $\text{MoS}_2$  peak: It appears to grow in from higher loss energy, 4.2 eV, in the category 5 films and to shift in energy as the films grow thicker. This would imply that the  $d_{z^2}$  orbital of Mo in the initial  $\text{MoS}_2$  is being affected by the substrate in a way that the HT films were not. However, spectral overlap is so great that this conclusion, although reasonable, must be regarded as speculative.

#### IV. CONCLUSIONS

The EEL spectra of thin AT and HT MoS<sub>2</sub> films on Si are evidence of an interface that is broad and chemically complex. Sulfur atoms from the plasma react with the native oxide on Si to produce sulfates; there may be more sulfates in AT than in HT films, although, as stated above, peak intensity is not a good indicator of the number of bonds. It is tempting to draw this conclusion, however, because it is well known that the number of oxygen-containing reactive sites on silica surfaces is lower on surfaces that have been heated in vacuum (HT) than on surfaces held near room temperature (AT).<sup>4</sup> It has been reported that 2000-Å HT MoS<sub>2</sub> films sputter-deposited on Si are oriented parallel to the substrate; such an orientation is probably due to the scarcity of active sites to force perpendicular orientation of the crystallites on such a surface.<sup>9</sup>

Elemental S is found in both thick and thin MoS<sub>2</sub> films, because of the way the films are made in the plasma. The S does not appear consistently (thin films of the same thickness category may or may not have elemental S), and it is not considered integral to the process of interface formation.

There is no evidence of MoO<sub>3</sub> in thin HT films, although it may be present in thin AT films. Unfortunately, the resolution of the spectra is not sufficient to bring out the details in the relevant AT-film spectra. Improved spectrometer resolution may help, although it is possible that the states are so broad or so closely spaced that the resolution is not spectrometer limited. The higher concentration of oxygen-containing active sites on the AT Si surfaces could enable some reaction with Mo as well as with S. On HT surfaces, all such sites (lesser in number) may have reacted with S before any Mo reaches the surface.

The initial MoS<sub>2</sub> in the thin HT films has its EELS peaks at exactly the same energies as the crystal, indicating no difference in bonding between them. The MoS<sub>2</sub> is not affected by the substrate, that is, there are no bonds between the film and substrate, which is consistent with the parallel orientation of 2000-Å-thick HT films on Si. The dearth of active sites to

induce perpendicular orientation by reaction with the edges of the  $\text{MoS}_2$  crystallites causes parallel orientation and no chemical bonding to the substrate.

In AT films, however, the 3.5-eV  $\text{MoS}_2$  peak appears to grow in from higher loss energy. This is a speculative observation and, if true, would imply that the  $d_{z^2}$  orbital of  $\text{MoS}_2$  is involved in bonding to the substrate, perhaps through Mo-S-O or Mo-O linkages.

Thus, the native-oxide-covered surface of Si (and presumably SiC and  $\text{Si}_3\text{N}_4$ ) is sulfated upon initial exposure to the plasma during deposition. Elemental S may be deposited also. In HT films,  $\text{MoS}_2$  is deposited on top of or beside the sulfates and is unaffected by them. In AT films, the initial  $\text{MoS}_2$  may be bonded through the sulfates or Mo-O linkages.

## REFERENCES

1. P. D. Fleischauer and R. Bauer, ASLE Trans. 30, 160 (1987).
2. M. R. Hilton and P. D. Fleischauer, Proc. Mater. Res. Soc. Symp. 5, held in Boston, MA, Nov/Dec 1988.
3. A. Koma and K. Enari, Inst. Phys. Conf. Ser. 43, 895 (1979).
4. A. Koma and K. Yoshimura, Surf. Sci. 174, 556 (1989).
5. J. R. Lince and P. D. Fleischauer, J. Vac. Sci. Technol. A5, 1312 (1987).
6. T. B. Stewart and P. D. Fleischauer, Inorg. Chem. 21, 2426 (1987).
7. P. D. Fleischauer and L. U. Tolentino, Proc. 3rd ASLE Int. Solid Lubr. Conf. ASLE SP-14 (1984), pp. 223-229; held in Denver, CO, 1984.
8. W. R. Salaneck, N. O. Lipari, A. Paton, R. Zallen, and K. S. Liang, Phys. Rev. B 12, 1493 (1975).
9. P. A. Bertrand, J. Mater. Res. 4, 180 (1989).
10. (a) H. Ibach and J. E. Rowe, Phys. Rev. B 9, 1951 (1974). (b) K. Fujiwara and H. Ogata, J. Appl. Phys. 48, 4360 (1977). (c) K. Fujiwara, H. Ogata, and M. Nishijima, Solid State Comm. 21, 895 (1977).